A PROCESS-BASED APPROACH TO SEDIMENT TRANSPORT IN THE YANGTZE ESTUARY

Ao Chu[1,2] Z.B. Wang[1,3] H.J. De Vriend[1,3] M.J.F. Stive[1]

A process-based model for the Yangtze Estuary is constructed to study the sediment transport in the estuary. The proposed model covers the entire tidal region of the estuary, the Hangzhou Bay and a large part of the adjacent sea. The dominant processes, fluvial and tidal, are included in the model. The calibration of the model against extensive flow, water level, salinity and suspended sediment data shows a good representation of observed phenomena. With the present calibrated and validated model, the residual flow field and the residual sediment transport field are obtained. The residual sediment transport pattern gives insight into the morphological behaviour of the mouth bars.

Key word: Yangtze Estuary; mouth bar; morphology; sediment transport; process-based model

INTRODUCTION

The morphological development of an estuary is affected by both marine influences, such as tides, waves, and the influx of saline water and marine sediments, and fluvial influences, such as flows of fresh water and fluvial sediment. Besides natural processes, anthropogenic activities, in the estuary as well as in the river basin, affect the evolution of the estuary. Based on the dominance of fluvial and marine (wave or tidal) processes, estuaries can be classified into different types (Dronkers 2005). The Yangtze Estuary is an estuary with fluvial deposits shaped by tide. Anthropogenic activities affecting the estuary are, for instance, dam construction and operation in the river basin, or the construction of the large-scale deep water navigation channel.

So far, most quantitative morphological predictions for the Yangtze Estuary rest mainly on data driven methods, e.g. the extrapolation of measured data (Wang 1986; Yu and Lou 2004; Hu 2005; Yang et al. 2005; Fan et al. 2006;Wang et al. 2007) and empirical input/output relationships (Ding and Shi 2000). Although this approach has been widely applied in studies on estuarine morphology, it is restricted by the availability and the quality of data. For example, the data taken after the construction of the Three Gorges Dam are as yet insufficient to support data-driven models of the response of the Yangtze Estuary. Yet, it is of utmost importance to be able to predict the morphological response of the estuary to climate change and anthropogenic activities, both from an economic and an ecological point of view. Process-based numerical modelling is an alternative approach. A process-based model describes the relevant physical processes starting from first physical principles (conservation laws), where necessary combined with empirical closure submodels (e.g. De Vriend et al. 1993). Dou et al. (1999) present a total sediment transport model for the Yangtze Estuary and hindcast the bathymetry change under a typhoon condition with it. Ding et al. (2003) apply a model for total sediment transport under waves and currents to study accretion/erosion in the navigation channel. Recently, Hu et al. (2009) use a 2D/3D hydrodynamic and sediment transport model to evaluate the development of a shoal in the estuary.

Morphodynamics is the mutual interaction of hydrodynamics, sediment transport and mobile-bed topography. Feedbacks between these components are essential to morphodynamic evolution. Yet, it is worthwhile to study sediment transport due to the various hydrodynamic processes, in order to have an impression of the relative importance of these processes.

One of the principal morphological features in the Yangtze Estuary is the mouth bar area, a shallow zone between river and sea. These mouth bars exhibit significant deposition at their seaward end, whence they tend to expand seawards (Hu 2005). The aim of this paper is to investigate the sediment transport in the Yangtze Estuary with a process-based model. The resulting residual transport field is used to explain the observed morphological changes in the mouth bar area.

[1] Faculty of Civil Engineering and Geosciences, Section of Hydraulic Engineering, Delft University of Technology, Stevinweg 1, 2628 CN, P.O. Box 5048, 2600 GA Delft, The Netherlands,
[2] College of Ocean, Hohai University, 1 Xikang Road, Nanjing 210098, China
[3] Deltares, Rotterdamseweg 185, P.O. Box 177, 2600 MH Delft, The Netherlands

THE YANGTZE ESTUARY MODEL

The proposed process-based model for the Yangtze Estuary is set up based on the Delft3D modeling system, which fully integrates the effects of waves, currents and sediment transport on morphological development in coastal, river and estuarine regions (Roelvink and van Banning 1994; Lesser et al. 2004). The modeling system consists of a few modules, such as flow, wave and morphodynamic, which can be coupled online. The description of those modules is reported in detail elsewhere (van Rijn 2000; Lesser et al. 2004).

Study area and model domain

The Yangtze Estuary is the outlet of the Yangtze River, which is the largest river in China. As shown in figure 1, the Yangtze River flows into the East China Sea with a connection to the Hangzhou Bay. The topography of the stretch from Xuliujing to the mouth, with a scale of 120 km long and 90 km wide, is characterized as three-stage bifurcation leading to four outlets, namely, North Branch (NB), North Channel (NC), North Passage (NP) and South Passage (SP).

The Yangtze Estuary is strongly influenced by the tide, which penetrates up to Datong (figure 1), about 640 km upstream from the mouth. The tidal current limit varies in the area between Jiangyin and Zhenjiang, which are 240 km and 360 km from the mouth, respectively. From Jiangyin to the sea, the width increases from 1.2 km to 91 km. In this area, the river flow slowing down and the mean tidal current velocity is about 1 m/s. Around the so-called mouth bar the fresh water from the river is mixed with the saline sea water, which results in an estuarine circulation and high turbidity. Suspended sediment flocculates, settles down and forms a mouth bar of some 50 km length.

Figure 2 shows the model domain, which covers the entire tidal region, the Hangzhou Bay and a part of the adjacent East China Sea. Instead of taking Jiangyin as the upstream river boundary, as was done in most previous models (Wu et al. 2006; Hu et al. 2009), the upper limit of the present model is taken at Datong. One of the advantages of this set-up is that the upstream boundary is free from tidal effects. Another advantage is that long time series of measured discharge and sediment concentration are available from Datong gauging station, which directly provide for the boundary conditions. The adjacent water bodies, the Hangzhou Bay and a part of the East China Sea, are important for exchanging water, sediment and other substance from the Yangtze Estuary. Especially the interchange between the Yangtze Estuary and the Hangzhou Bay cannot be neglected (Du 2007; Huang 2007). In addition, the open boundary of the model should be far away from the study area.

The model domain extends over some 800 km long in longitude direction and some 400 km in latitude direction. For computational efficiency, domain decomposition is applied. The model is separated into two grids at Jiangyin cross section. Both are boundary-fitted orthogonal curvilinear grids. The upper grid, from Datong to Jiangyin, has 949 grid points along the river and 24 in the transverse direction. It covers the 400 km long river reach with grid resolution varying from 100 m to 1.5 km. Only 2D simulation is applied to the upper domain. The lower grid covers area from Jiangyin to the sea side boundary with an area of 400×300 km (figure 2). This grid consist of 305×199 grid points with a high resolution near the outlets and coarser towards the open sea boundary. The grid size ranges from 200 m to 6 km. 2-D and 3-D simulations can be made by applying a single or multiple layers in the vertical.

The bathymetry of the Yangtze Estuary model is also shown in figure 2. The bathymetry data is based on maps measured in 2002. The depths at the grid points are obtained by triangular interpolation.

Driving forces

Classified as an estuary with fluvial deposits shaped by tide, the Yangtze Estuary has the fluvial sediment supply is its main sediment input. As mentioned above, the upstream boundary of the present Yangtze Estuary model is set at the tidal limit, Datong, where a long time series of measured data is available. By specifying the monthly or daily total discharge with the associated sediment concentration, the fluvial input can be defined.

The tide is one of the main driving forces shaping the morphology of the Yangtze Estuary. The astronomic tidal constituents are prescribed at the open sea boundary.

Swell due to typhoons, as well as the locally generated wind waves, are also important forces for the morphological development of the Yangtze Estuary, especially for the event-driven changes (Hu et al. 2009). In this paper, we focus rather on long-term trends and choose not to include wave effects.

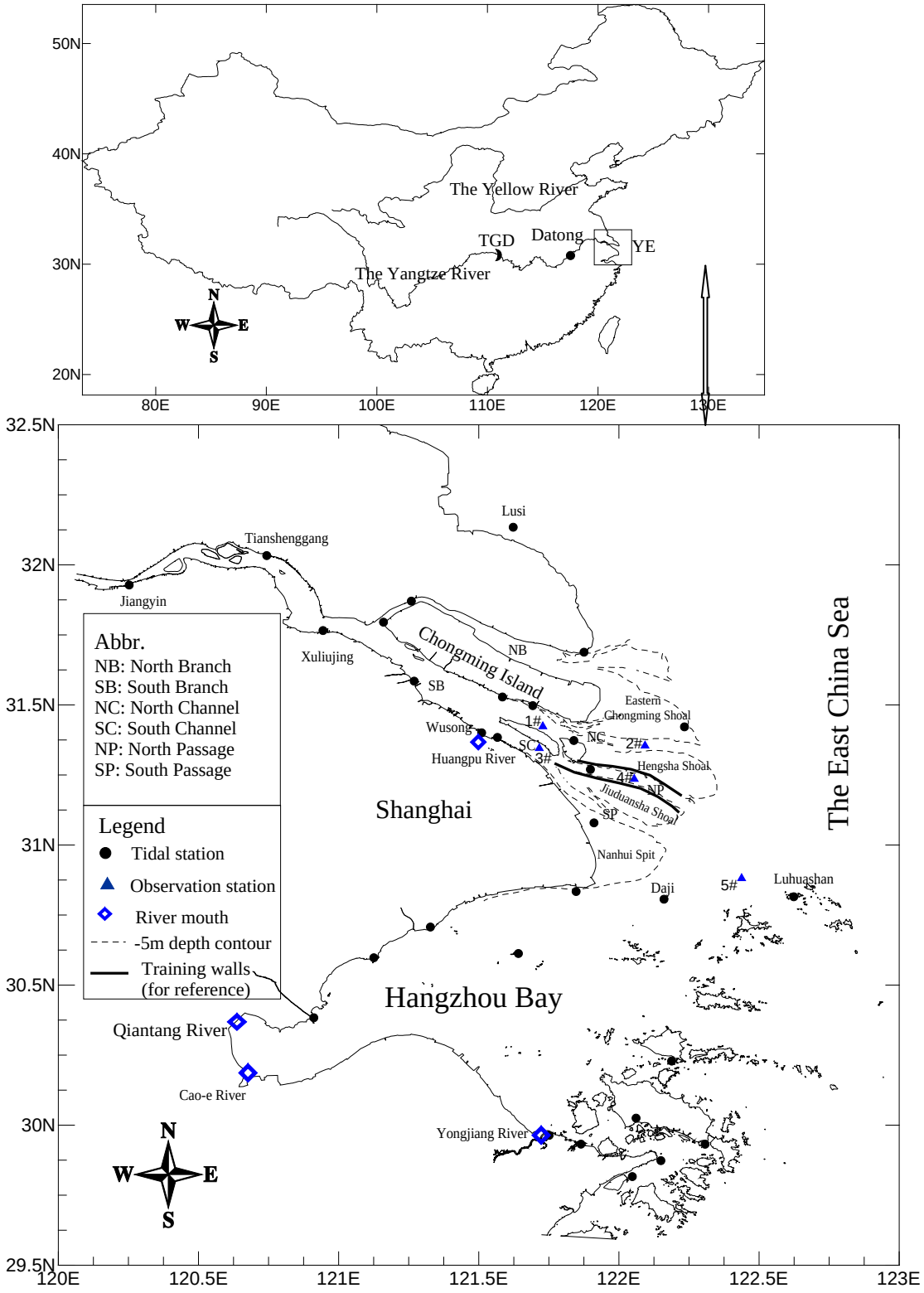

Figure 1. The study are and the layout of the Yangtze Estuary.

Salinity is important in the Yangtze Estuary, not only via density currents, but also via the flocculation of the fine cohesive sediment. The seasonal cycle in the river discharge and the spring-neap cycle of the tide cause long-term variations of the salinity distribution which may have

morphological effects on the timescale considered. Therefore, salinity is also included in the present model.

Boundary conditions

Measured monthly mean discharge at Datong are available since the 1950s', daily values over the last ten years. Besides the Yangtze River, there are four other major rivers (figure 1), Qiantang River, Huangpu River, Cao-e River and Yongjiang River, flowing into the model domain. Table 1 shows the yearly average discharges of the major rivers in the domain. Although the Qiantang River has only 5% of discharge of the Yangtze River, it still has a considerable size and strong tidal current with the famous tidal bore occurring. Here the water level is defined at Haining with astronomic tidal constants as boundary condition. As an alternative, a weakly reflective boundary condition has been applied at Haining (Wang 1995). As neither the discharges nor the magnitudes of the other three rivers are comparable to the Yangtze River (see table 1 and figure 1), these three rivers are treated in the model as fresh water sources with average discharges.

Table 1. River discharge in the domain (Partly from Wang 1995).

River	Discharge(m^3/s)
Yangtze River	29000
Qiantang River	1468
Huangpu River	318
Cao-e River	82
Yongjiang River	91

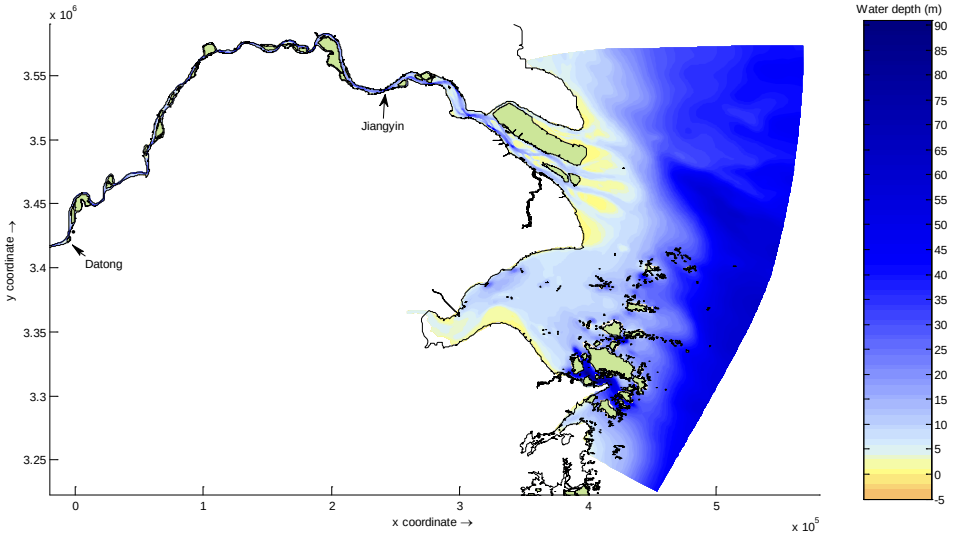

Figure 2. Model domain coverage and water depth.

At the open sea boundary, the astronomic tidal constituents are specified to represent the tidal force. This means that the mean water levels as well as the tidal constituents along the boundary have to be known. However, very limited information is available on both. No information is available for the mean water level along the boundary. Fortunately, most of the boundary is in the open sea, where the mean water level is close to mean sea level. Slight variations about the mean water level can be adjusted by calibration. The ideal way to obtain the tidal constituents along the boundary is using result of a larger ambient model. At present the only information available stems from the China Sea Model (Zhang 2005), which gives the propagation maps of the M2 and K1 tides. An estimation of M2 and K1 tides at the open sea boundary is determined by digitizing those co-tidal maps. Besides M2 and K1 tides, other tidal constituents are also important in the Yangtze Estuary. Tidal analysis of water level

time series at several stations in the estuary shows that S2, N2, K2, K1, P1 and O1 have larger amplitudes than other constituents. To determine those tidal constituent at the open sea boundary, linear regression with one free parameter (Wang 1995) has been used to obtain the relationship of tidal constants (amplitude and phase lag) between every two constituents. The relationships obtained from the regression analysis are shown in table 2.

Table 2. Relationship in amplitude and phase lag between two tides.

Amplitude (m)	Phase lag (degree)
S2=0.345M2	S2=M2+45
K2=0.26S2	K2=S2-2.8
N2=0.142M2	N2=M2-16.3
P1=0.20K1	P1=K1+5.0
O1=0.265K1	O1=K1-50

The sediment concentration at open boundaries is specified to represent the sediment input to the estuary together with the discharge. The measured average sediment concentration (monthly or daily) is available at Datong. For the other rivers, the yearly mean concentration is specified. At the open sea inflow boundary, an approach of the flow carrying same sediment concentration as computed in the interior of the model is applied.

The salinity at the open sea boundary is determined from the maps of the seasonal distribution in the East China Sea (Guo et al. 2004).

Sediment

The main sediment source of the Yangtze estuary is the Yangtze River. Based on the data of 1950~2001 at Datong, the average sediment load is about 430 million t/year, of which 90% suspended load with an average concentration of 0.48 kg/m^3. In the past two decades, the total sediment load of the river decreases rapidly: from 471 million ton/year (1950~1989), via 346 million ton/year (1900~2000) to 226 million ton/year (2001~2004).

Yun (2004) indicates that the mean diameter of the suspended sediment at Datong is about 10~30μm, which is mainly fine silt and clay with cohesive behaviour. The mean diameter of the suspended sediment in the reach from Datong to the South Branch remains of the same order of magnitude as that at Datong. Around the mouth of the estuary, the flood/ebb current speed is less than in the upper reach, which results in settling of the coarser suspended particles. Therefore, the diameter of the suspended sediment in the mouth becomes finer than further upstream, with a mean diameter about 8μm. The diameter of the bed load also decreases along the main channel, again due to the decreasing velocities. In the upstream reach down to Hengsha it is mainly fine and medium sand with a mean diameter larger than 100μm. From Hengsha to the mouth of the estuary, the mean diameter of the bed material is smaller than 30μm, with coarser sediment at the bed around the mouth of North Channel, Hengsha Shoal, middle North Passage and upper part of Jiuduansha Shoal and with finer sediment at the bed around the shoals in South Passage. Further seawards, the mean diameter of the bed material becomes much finer. Wan et al. (2003) present similar sediment characteristics. In summary, the sediment transport in the Yangtze Estuary involves both suspended load and bed load. The suspended load consists of very fine cohesive particles, typically in the range 10~30μm. The bed load is much coarser, with a typical diameter of about 60~180μm. Therefore, two types of sediment are included in the Yangtze Estuary model. One is fine sand of 120μm to represent the bed load, and the other is fine cohesive sediment of 20μm.

The transport of suspended sediment is calculated by solving the advection-diffusion equation for suspended sediment, coupled online with the hydrodynamics. Important submodels concern the erosion and deposition fluxes at the bed. To calculate these quantities different formulations should be applied, because the two types of sediment behave differently. For the coarse noncohesive sediment, Van Rijn's transport formula (van Rijn 2007a, 2007b; van Rijn et al. 2007) is used. For the fine cohesive sediment the Partheniades-Krone formulation (Partheniades 1965) is used to calculate the exchange fluxes between bed and flow. The cohesive sediment erosion and deposition can be represented as

$$E=M\,S(\tau_{c,b}, \tau_{cr,e}) \qquad (1)$$

$$D=\omega_s\, c_b\, S(\tau_{c,b}, \tau_{cr,d}) \quad (2)$$

$$c_b=c(z=\Delta z_b/2,t) \quad (3)$$

in which:

E: erosion flux (kg/m^2/s)

M: erosion parameter (kg/m^2/s)

$S(\tau_{c,b}, \tau_{cr,e})$: erosion step function:

$$S(\tau_{c,b}, \tau_{cr,e})=(\tau_{c,b}/\tau_{cr,e}-1) \quad \text{when } \tau_{c,b} > \tau_{cr,e}$$

$$=0 \quad \text{when } \tau_{c,b} \le \tau_{cr,e} \quad (4)$$

D: deposition flux (kg/m^2/s)
ω_s: (hindered) settling velocity (m/s)
c_b: average sediment concentration in the near-bottom computational layer
$S(\tau_{c,b}, \tau_{cr,d})$: deposition step function:

$$S(\tau_{c,b}, \tau_{cr,d}) = (1-\tau_{c,b}/\tau_{cr,d}) \quad \text{when } \tau_{c,b} \le \tau_{cr,d}$$

$$=0 \quad \text{when } \tau_{c,b} > \tau_{cr,d} \quad (5)$$

$\tau_{c,b}$: mean bed shear stress due to current (N/m^2)
$\tau_{cr,e}$: critical erosion shear stress (N/m^2)
$\tau_{cr,d}$: critical deposition shear stress (N/m^2)

In this study, it is assumed that erosion and deposition can occur simultaneously (Winterwerp and Kesteren 2004). To that end, the deposition rate D is given by

$$D=\omega_s\, c_b \quad (6)$$

In this case, the reference concentration follows from taking the deposition flux equal to the erosion flux:

$$c_b=M\,(\tau_{c,b}/\tau_{cr,e}-1)/\omega_s \quad (7)$$

Eq. (7) shows that the reference concentration is proportional to the erosion parameter and the excess bed-shear stress, and inversely proportional to the critical erosion shear stress and the settling velocity. The bed-shear stress follows from the hydrodynamic computation. The erosion parameter is a calibration factor. The critical bed shear stress for fine cohesive sediment can be influenced by cohesive particle-particle interaction effects ($\varphi_{cohesive}$), by packing effects ($\varphi_{packing}$) and by biological and organic material effects (φ_{bo}), represented in (van Rijn 2007a)

$$\tau_{cr,e}=\varphi_{bo}\ \varphi_{packing}\ \varphi_{cohesive}\ \tau_{cr,o} \quad \text{for particles } <62\mu m \quad (8)$$

where $\tau_{cr,o}$ is the critical bed shear stress for erosion of cohesive particles. For sediment of 20μm, the critical erosion shear stress is about 0.1 N/m^2. The settling velocity for the fine cohesive sediment can be calculated as (van Rijn 2007b)

$$\omega_s=\varphi_{floc}\ \varphi_{hs}\ \omega_{s,o} \quad (9)$$

where φ_{floc}=flocculation factor; φ_{hs}=hindered settling factor; and $\omega_{s,o}$ = settling velocity of a single suspended particle in clear water. The flocculation factor (for particles finer than 62μm and salinity ≥ 5ppt) is proposed to be represented by (van Rijn 2007b)

$$\varphi_{floc}=[4+\lg(2c/c_{gel})]^{\alpha} \quad (10)$$

where $\alpha=(d_{sand}/d_{50})-1$, d_{sand}=62μm. And the hindered settling factor is given by (van Rijn 2007b)

$$\varphi_{hs}=(1-0.65c/c_{gel})^5 \quad (11)$$

where $c_{gel}=(d_{50}/d_{sand})c_{gel,s}$ with $c_{gel,s}$ =1722 kg/m3 for pure sand and c=sediment concentration in water. In this study the settling velocity of a single suspended particle of 20μm in fresh water is taken

0.37 mm/s. Flocculation is supposed to be fully active for a salinity value larger than about 5 ppt, yielding an effective settling velocity of 1.85 mm/s.

Model performance

The model is calibrated against an extensive set of hydrodynamic data at several locations throughout the model domain. Adjustments of the calibration parameters have been made to obtain the good agreement between simulation results and measurement. In the following, comparisons of measured and computed tidal constituents (water levels), current velocity, current direction, salinity and sediment concentration at stations around the mouth bar are presented.

Table 3 gives the comparison between measured tidal constituents (amplitude and phase lag) and those computed with the 2DH model at the stations shown in figure 1. The measured constituents are obtained by applying tidal analysis on the time series of measured water levels at each station. The same analysis technique is applied to the computed water levels. As appears from table 3, the ratios between the computed and the measured amplitudes are close to 1 for all constituents, with most deviations less than 5%.

Table 3. Comparison between modeled and measured tidal constants ($R_A=A_{calculated}/A_{measured}$; $\Delta G=G_{calculated}- G_{measured}$).

Station	M2		S2		N2		K2		K1		P1		O1	
	R_A	ΔG	R_A	ΔG	R_A	ΔG	R_A	ΔG	R_A	ΔG	R_A	ΔG	R_A	ΔG
Tianshenggang	1.02	3.1	0.91	1.2	1.01	4.0	0.93	6.8	1.02	2.6	0.96	0.8	0.97	1.9
Xuliujing	1.01	3.4	0.94	0.0	1.06	3.1	0.94	7.0	1.00	2.2	1.04	-5.5	1.02	2.9
Wusong	1.06	-2.1	1.04	0.9	1.00	-2.5	0.98	-0.4	1.02	-1.4	1.04	-1.6	1.05	-0.3
Daji	1.00	-1.4	1.09	2.9	1.04	-0.4	0.98	2.6	0.98	-1.1	0.92	7.6	0.96	2.5
Luhuashan	0.96	-0.7	1.00	3.0	0.95	-1.6	0.91	4.1	0.94	-1.6	0.87	3.1	0.92	0.9

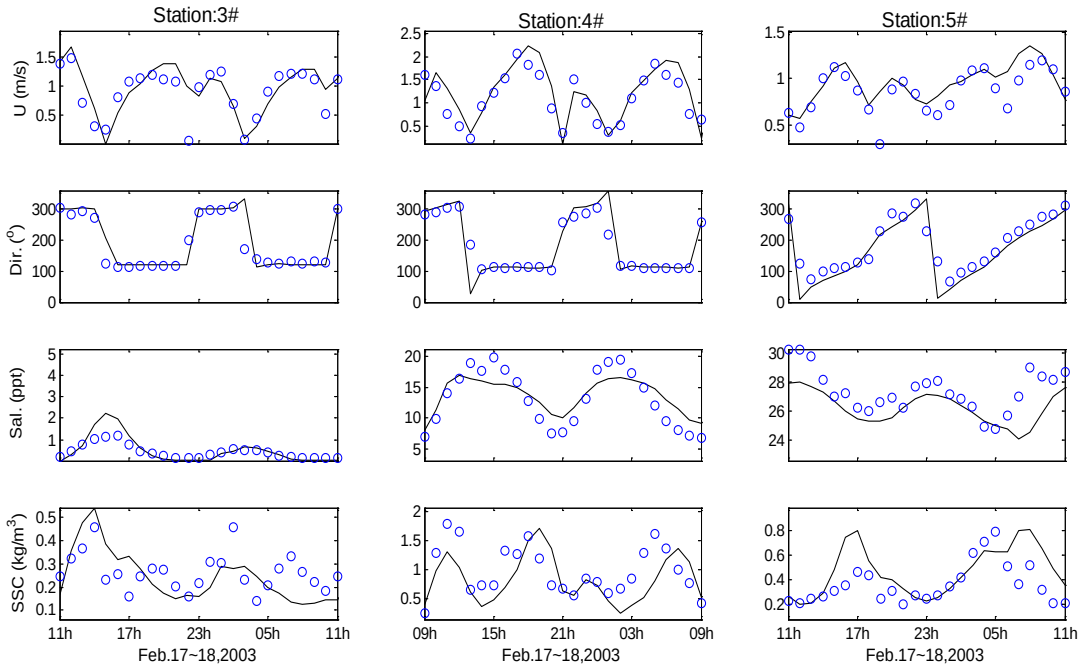

Figure 3. Comparison between measured (symbol) and computed (line) results at stations 3#, 4# and 5# (From top to bottom: current speed, current direction, salinity and suspended sediment concentration).

The measured and computed current velocity, current direction, salinity and sediment concentration at three stations (see figure 1 for their locations) are compared in figure 3. It shows that also the current velocity and direction are represented well. The salinity and sediment concentration

results exhibit larger differences, which may be caused by processes not included in the model, such as density currents, wind and waves. Nonetheless, the ranges of variation are in the right order of magnitude. Therefore, the model is claimed to also represent the salinity and the sediment concentration in the estuary.

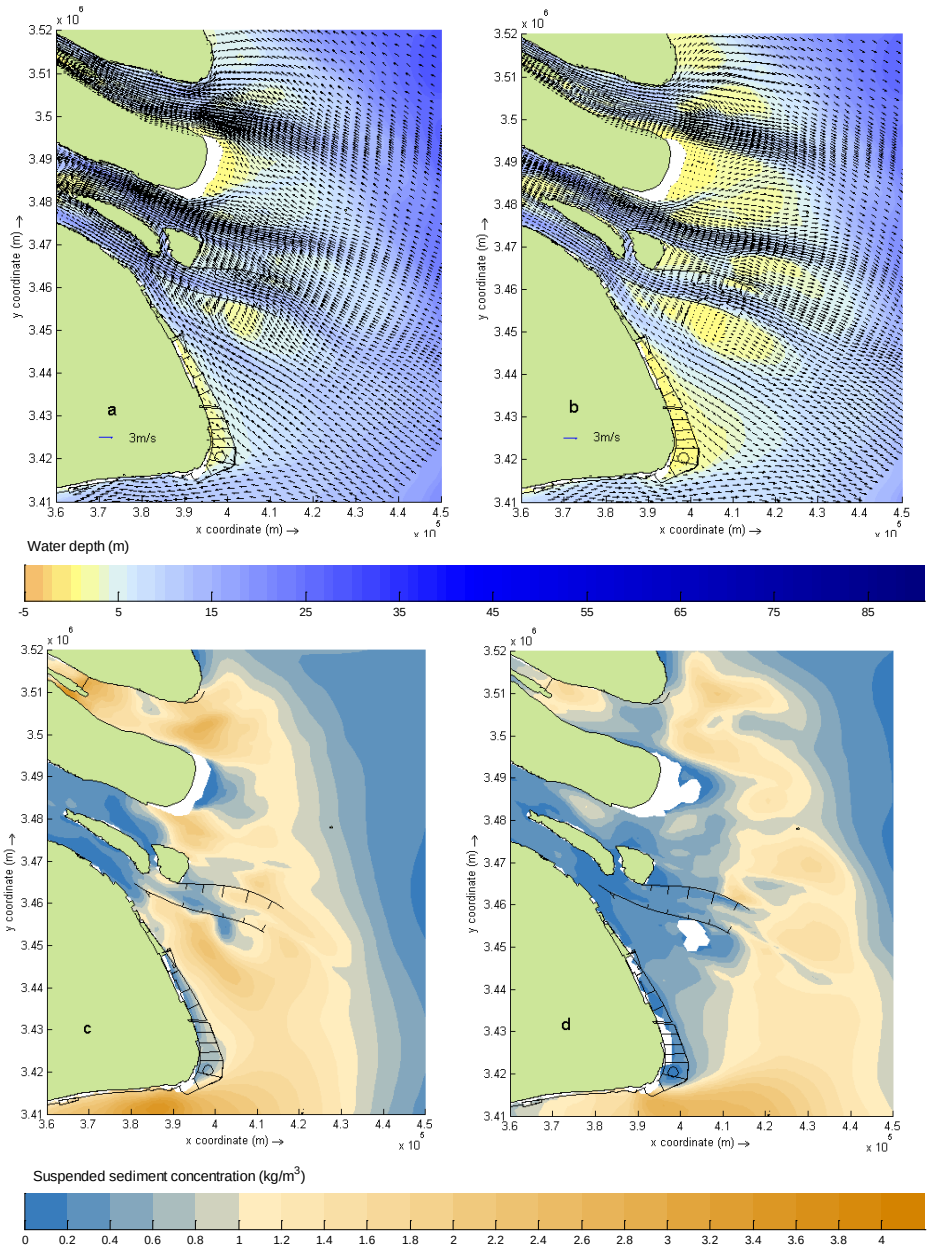

Figure 4. Current velocity and suspended sediment distribution around the mouth bar in the Yangtze Estuary, February 2003 (a, b: velocity fields during maximum flood and ebb; c, d: sediment concentration fields during maximum flood and ebb).

Figures 4a and 4b show the horizontal velocity field during maximum flood and ebb. The locations of the four outlets of the estuary are evident. On the shoals the current velocity at maximum flood is smaller than at maximum ebb, due to the differences in water depth associated with the vertical tide. The flow fields also show that the converging effects of shoals (or training walls and groins) are well represented. Figures 4c and 4d show the sediment concentration fields, also at maximum flood and ebb. Clearly, the turbidity maximum coincides with the mouth bar area. The high concentration zone at maximum flood lies more landward than that at maximum ebb, since it moves with the tidal

current. The phenomena shown in figure 4 agree well with observations (Chen et al. 1995; Xue et al. 1995) and other model results (Hu et al. 2009).

RESIDUAL FLOW AND TRANSPORT FIELDS

The morphological development of the mouth bar in the Yangtze Estuary has been the subject of extensive studies. Yang et al. (2001) derive the temporal variation of bed level changes in the South Passage from 23 bathymetric surveys. They point out that the bed level change is correlated to the discharge at Datong. Wu et al. (2002) apply GIS to analysis 10 sea maps of the Yangtze Estuary in the period 1842 - 1997 and indicate that the mouth bar is expanding seawards, with deposition occurring at Jiuduansha shoal, Hengsha Shoal and Eastern Chongming Shoal. Hu (2005) also analyses historical sea maps and obtains the mouth bar behaviour over the last 150 years. He points out that Hengsha Shoal and Jiuduansha Shoal are expanding in southeasterly direction. In addition to these data-analyses, the computed residual flow and sediment transport fields can give insight into the mechanisms underlying the mouth bar development.

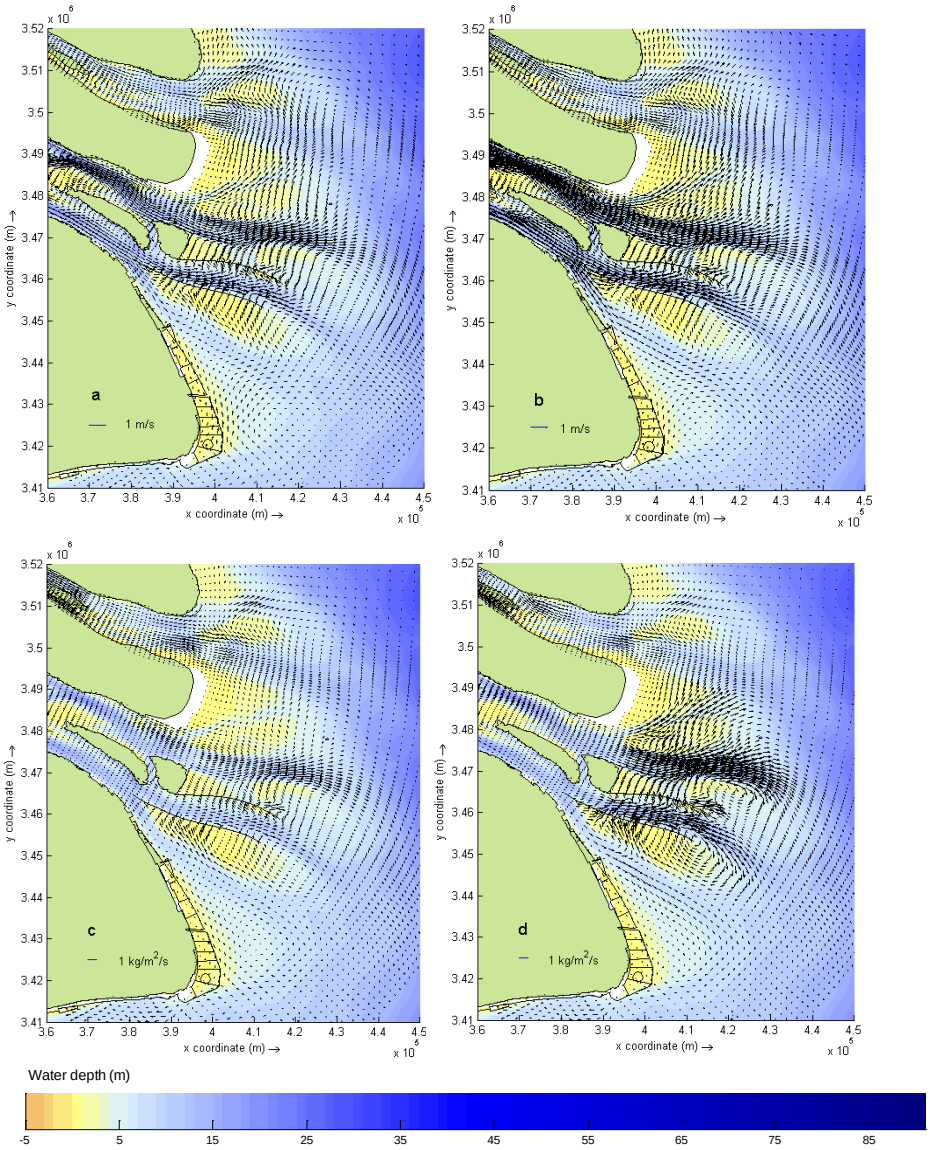

Figure 5. Residual flow field and residual sediment transport field (a, b: residual flow fields during spring tide in February and July 2003; c, d: residual sediment transport fields during spring tide in February and July 2003) .

As the tide in the Yangtze Estuary is predominantly semidiurnal (M2), a cycle period of 24 hours and 50 minutes is chosen to determine the residual fields. Simulations have been carried out in the dry season (February 2003) and in the flood season (July 2003). The residual flow and sediment transport fields for a spring tide, mean tide and neap tide in those seasons are computed. Figure 5 gives the results for spring tide, showing that the overall patterns of the residual flow field and the residual sediment transport field are similar, yet different. The residual flow velocity is of the order of 10~30 cm/s, which agrees with results based on field measurements reported in the literature (Chen et al. 1995; Xue et al. 1995; Kong et al. 2007).

Figure 5 clearly shows that the transport at the seaward edge of the mouth bar, especially around the eastern parts of Jiuduansha Shoal and Hengsha Shoal, rapidly decays and forms two large-scale gyres, which favours deposition. Thus the shoals tend to expand seawards, which agrees with observations (Wu et al. 2002; Hu 2005). The residual sediment transport pattern in the South Passage differs between the seasons, as a result of the difference in discharge. The residual transport over Jiuduansha Shoal is directed towards the navigation channel (located between the two training walls) and drops in the channel, thus giving rise to serious accretion in the channel, as has been reported.

CONCLUSION AND FURTHER RESEARCH

Using Delft3d, a process-based model for the Yangtze Estuary was set up in this study. Model calibration results shows the model performs well in representing the hydrodynamics and the sediment transport in the estuary. The residual flow and the residual sediment transport due to fluvial and tidal processes are obtained based on the model result. The residual sediment transport pattern is used to get insight into the morphological development of the estuarine mouth bar. For the present morphology, the residual transport pattern in the Yangtze Estuary shows two large-scale gyres at the seaward edge of the mouth bar. This explains the observed seaward expansion of the mouth bar. The residual transport pattern in the middle of the navigation channel predicts serious accretion, as observed in reality. Therefore, in addition to the analysis of observed flow and transport phenomena, the proposed model also gives insight into the morphodynamics of the estuary.

Due to the complexity and highly dynamic nature of the Yangtze Estuary, there is lot of work remaining to improve the model. For instance, density currents strongly affect the residual sediment transport field. Therefore, 3D simulations accounting for density currents will be applied to further investigate the sediment transport in the estuary. Other relevant processes (e.g. wind, wave, etc.) will also be considered. A next step will be to include morphodynamic feedback.

Human interventions, especially the Three Gorges Dam constructed upstream, directly influence the flow regime and the associated sediment transport. The impact of this kind of interventions urgently needs to be assessed. Comprehensive field campaigns together with long term monitoring are needed to supply data for model calibration and process analysis.

ACKNOWLEDGEMENT

The first author is financially supported by the China Scholarship Council and co-sponsored by WWF in the “Support to the Estuary Version Development for a Healthy and Sustainable Yangtze Estuary” project, under contract no. CN091101-3514 and by Youth Found of HHU-2010B03314.

This work was additionally supported by the project ‘Effects of human activities on the eco-morphological evolution of rivers and estuaries’ financed by the Dutch Royal Academy of Sciences (KNAW) and the Chinese Ministry of Science and Technology within the framework of the Programme of Scientific Alliances between China and the Netherlands.

REFERENCES

Chen Z., Wu S., Xia D., Xie Q., Chen F., Hu H., Zhan J., and He B. 1995. Chinese Bay, *China Oceanpress*, pp. 142-145, vol.14 (in Chinese).

De Vriend H.J., Capobinaco M., Chesher T., de Swart H.E., Latteux B., and Stive M.J.F. 1993. Approach to long-term modelling of coastal morphology: a review, *Coastal Engineering*, pp 225-269.

Ding P. and Shi F. 2000. Prediction Model for the Erosion and Accretion in the South Passage of the Yangtze Estuary, *Research report* (in Chinese).

Ding P., Hu K, Kong Y. and Zhu S. 2003. Numerical simulation of total sediment under waves and currents in the Changjiang Estuary, *Acta Oceanologica Sinica*, Vol.5, pp113-124 (in Chinese).

Dou X., Li T. and Dou G. 1999. Numerical model study on total sediment transport in the Yangtze River estuary, *Hydro-Science and Engineering*, Vol.2, pp31-41(in Chinese).

Dronkers, J. 2005. Dynamics of coastal systems, *Advanced Series on Ocean Engineering*, vol. 25, World Scientific, Singapore.

Du P. 2007. Sediment Transport Research in Yangtze Estuary and Hangzhou Bay, *PhD dissertation*, East China Normal University (in Chinese).

Fan D., Guo Y., Wang P. and Shi, J.Z. 2006. Cross-shore variation in morphodynamics processes of an open-coast mudflat in the Changjiang Delta, China: With an emphasis on storm impacts, *Continental Shelf Research* , 26(2006), pp.517-538.

Hu H. 2005. Evolution characteristics and trend of the shoals around the second and third generation alluvial islands in Changjiang Estuary, *MSc thesis*, East China Normal University (in Chinese).

Hu K., Ding P., Z.B. Wang and Yang S. 2009. A 2D/3D hydrodynamic and sediment transport model for the Yangtze Estuary, China, *Journal of Marine Systems*, Vol.77, pp 114-136.

Huang G. 2007. Study on the Character of Flow and Sediment Exchange and Transport between Changjiang Estuary and Hangzhou Bay, *MSc. thesis*, East China Normal University (in Chinese).

Guo B., Huang Z., Li P., Ji W., Liu G. and Xu J. 2004. Marine environment of the Chinese Coast and the adjacent seas, *China Oceanpress*, pp.38-47 (in Chinese).

Kong Y., Ding P. and He S. 2007. Analysis on the characteristics of residual flow in sea adjacent to the Yangtze Estuary, *Advance in Marine Science*, vol.25, No.4 (in Chinese).

Lesser G.R., Roelvink J.A., Kester J.V. and Stelling G.S. 2004. Development and validation of a three-dimensional morphological model, *Coastal Engineering*, vol.51, pp.883-915.

Partheniades E. 1965. Erosion and Deposition of Cohesive Soils, *Journal of the Hydraulic Division*, ASCE, no. HY1,ol 91.

Roelvink J.A. and Van Banning G.K.F.M. 1994. Design and development of Delft3D and application to coastal morphodynamics, *Proc. of Hydroinformatics '94 Conf*, Delft.

Van Rijn, L.C. 2000. General View on Sand Transport by Currents and Waves: Data Analysis and Engineering Modeling for Uniform and Graded Sand TRANSPOR2000 and CROSMOR2000 Models, *Report*, WL Delft Hydraulics.

Van Rijn L.C. 2007a. Unified View of Sediment Transport by Currents and Waves. I: Initiation of Motion, Bed Roughness, and Bed-Load Transport, *Journal of the Hydraulic Division*, ASCE, Vol. 133, No.6, 649-667.

Van Rijn L.C. 2007b. Unified View of Sediment Transport by Currents and Waves. II: Suspended Transport, *Journal of the Hydraulic Division*, ASCE, Vol. 133, No.6, 668-689.

Van Rijn L.C., Walstra, D.J.R., and Van Ormondt, M. 2007. Unified View of Sediment Transport by Currents and Waves. IV: Application of Morphodynamic Model, *Journal of the Hydraulic Division*, ASCE, Vol. 133, No.7, 776-793.

Wan X., Li J., He Q., Xiang W. and Wu H. 2003. Water and sediment fluxes in the middle and lower Yangtze River, *Journal of sediment research* (in Chinese).

Wang S. 1986. The evolution characteristics of the Changjiang Estuary, *Journal of Sediment Research*, Vol.04: pp1-12 (in Chinese).

Wang, Z.B. 1995. Hangzhou Bay Environmental Study Hydrodynamic Modeling, *Report*, WL Delft Hydraulics.

Wang Y., Ridd P.V., Wu H., Wu J. and Shen H. 2007. Long-term morphodynamics evolution and equilibrium mechanism of a flood channel in the Yangtze Estuary (China), *Geomorphology*, Vol. 99, pp.130-138.

Winterwerp J.C. and Kesteren W.G.M.V. 2004. Introduction to the physics of cohesive sediment in the marine environment. *Developments in Sedimentology*, 56. Elsevier, 466 pp.

Wu H., Shen H., Hu H., Zhang L., and Huang Q. 2002, GIS supporting study on calculation of amount of siltation and erosion in mouth bars of the Changjiang Estuary, *Acta Oceanlogica Sinica*, Vol.23, No.2.

Wu H., Zhu J. Chen B. and Chen Y. 2006. Quantitative relationship of runoff and tide to saltwater spilling over from the North Branch in the Changjiang Estuary: A numerical study, Estuarine, *Coastal and Shelf Science*, vol.69, pp.125-132.

Xue H., Xie J., Hu F., and Zhang H. 1995. Hydrology of the Chinese coast, *China Oceanpress*, (in Chinese).

Yang S., Zhao Q., Ding P. and Xie W. 2001. seasonal changes in bed levels of the passage in the mouth bar area of the Yangtze (Chanjiang) River, *Resources and environment in the Yangtze Basin*, Vol.10, No.3 (in Chinese).

Yang S.L., Zhang J., Zhu J., Smith J.P., Dai S.B., Gao A. and Li P. 2005. Impact of dam on the Yangtze River sediment supply to the sea and delta intertidal wetland response, *Journal of Geophysical Research*, Vol. 110, F03006.

Yu Z. and Lou F. 2004. The evolvement characteristics of Nanhuizui foreland in the Changjiang Estuary, China, *Acta Oceanologica Sinica*, Vol. 26, No.3 pp47-53(in Chinese).

Yun C. 2004. Recent development of the Changjiang estuary, *China Oceanpress*, (in Chinese).
Zhang W. 2005. Numerical Modeling of Tides Wave in Margin Seas near China, *MSc thesis*, Hohai University (in Chinese).